Analysis of tropospheric structure from multi-station PPP-analysis

Franziska Kube and Steffen Schön
Institut für Erdmessung | Leibniz Universität Hannover

Leibniz Universität Hannover

Motivation and Introduction

Tropospheric Refraction

- Refractivity variations in Neutral Atmosphere form a significant error source for space-geodetic techniques such as Global Navigation Satellite Systems (GNSS) or Very Long Baseline Interferometry (VLBI)
- At the same time refraction variations are valuable as signal, which can be used to enhance the modelling of neutrospheric refraction
- Especially micro-scale meteorological phenomena (turbulent properties) are little studied and not yet considered in routine analysis, such as Reference Frame determination

Purpose of this study

- Investigate the spatial structure of the troposphere from distributed GPS and VLBI stations at the Geodetic Observatory Wettzell, Germany, by means of geostatistics
- Develop a strategy to find a suitable model to the describe spatial structure by including observations of different periods of time
- Check feasability of estimating Zenith Wet Delays (ZWDs) for an arbitrarily choosen epoch and line of sight (GPS or VLBI) from an interpolated surface of ZWDs

Data

- GPS L3 carrier phase residuals and ZWDs from 4 stations at Wettzell Observatory (*WTZR*, *WTZS*, *WT33*, and *WT27*) @1Hz from daily PPP Kalman Filter solution for 3 days in Feb. 2015 (for setting see [Kube and Schön, 2016])
- VLBI (*RTW*) ZWDs @30min

Finally 18 hours of data on DoY 50 2015 from both techniques were used for this study.

Analysis steps and Methods

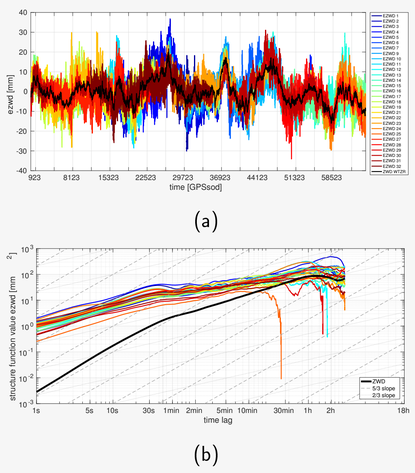

(a) (b)

Fig. 1: Equivalent ZWD (EZWD) for WTZR (a) and corresponding temporal structure funtions (b).

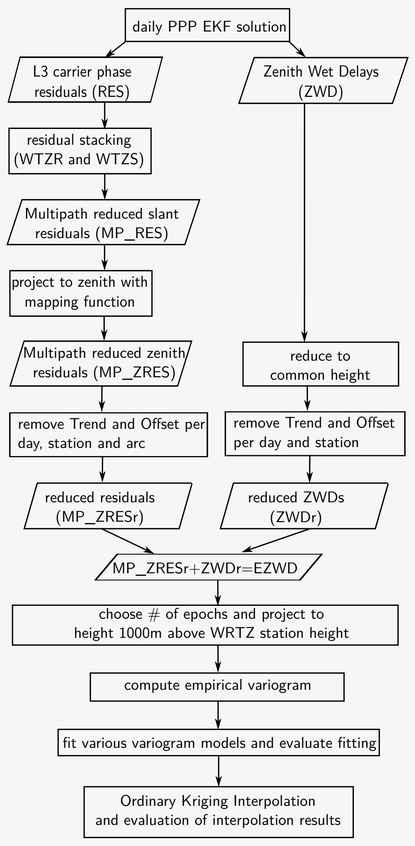

Fig. 2: Flowchart of the estimation of a tropospheric surface from Zenith Wet Delays and PPP residuals.

Preprocessing

- GPS residual stacking according to [Fuhrmann et al., 2015] in order to reduce the multipath influence. Since permanent GPS observations are not available for *WT33* and *WT27*, multipath reduction was only possible for *WTZR* and *WTZS*
- Reduction of VLBI and GPS ZWDs to commom height and removing trend and offset from residual and ZWD time series
- Computation of GPS Equivalent ZWDs (**EZWD**s) by mapping the residuals to the zenith and adding the ZWD, see Fig. 1(a) - residuals contain mainly turbulence, since all other remaining effects are carefully modelld in our PPP algorithm, see Fig. 1(a)
- Choosing VLBI ZWD epochs (36 epochs @30min) as reference epochs
- Projecting GPS EZWDs and VLBI ZWD to plane 1000m above Wetzell, see Fig. 3(a) and 3(b)

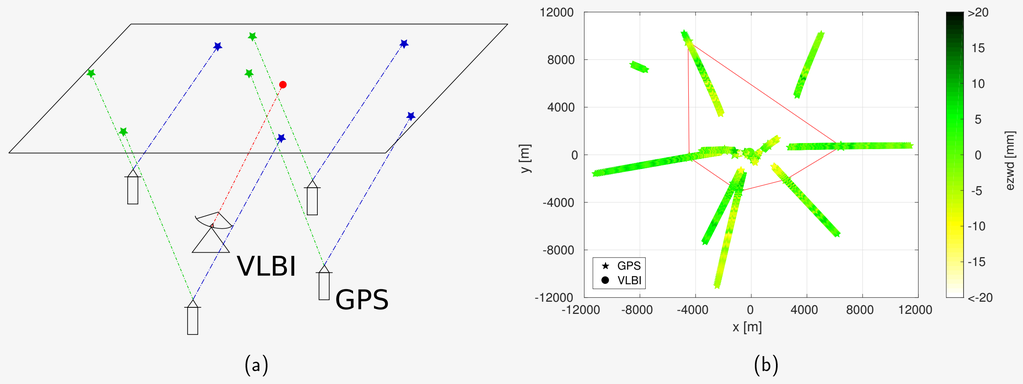

(a) (b)

Fig. 3: Schematic representation of EZWDs projected to plane @1000m height (a) and EZWDs in the plane for sample epoch GPSsod 12523 with convex hull (red line) and EZWDs of ± 15min (b).

Variogramm Computation and Fitting

- Setting up empirical variograms by computing semivariances $\gamma(h) = \frac{1}{2n}\sum_{i=1}^{n}[EZWD(x_i) - EZWD(x_i + h)]$ with lag distance h between points in plane, n the number of points within a distance class, here we used 300m, and x_i, the local coordinate in the plane. Plotting the empirical semivariances against the distance shows the spatial variability of EZWDs, see squares in Fig. 4(b) and Fig. 4(c).
- Fitting variogram modells to the data [Stein, 1999] by means of least squares fit: Linear Model (1), Exponential Model (2), Mátern Model with Exponent $\nu = 1/3$ (3)

$$\gamma^{lin}_{a,b}(h) = \begin{cases} 0, & \text{if } |\mathbf{h}| = 0, \\ c_0 + b\left(\frac{|\mathbf{h}|}{a}\right), & \text{if } 0 \leq |\mathbf{h}| \leq a. \\ c_0 + b, & \text{else,} \end{cases} \quad (1)$$

$$\gamma^{exp}_{a,b}(h) = \begin{cases} 0, & \text{if } |\mathbf{h}| = 0, \\ c_0 + b\left(1 - \exp\left(-\frac{|\mathbf{h}|}{a}\right)\right), & \text{else,} \end{cases} \quad (2)$$

$$\gamma_{a,b,\nu}(h) = \begin{cases} 0, & \text{if } |\mathbf{h}| = 0, \\ c_0 + b\left(1 - \frac{1}{2^{(\nu-1)}\Gamma(\nu)}\left(\frac{2\sqrt{\nu}|\mathbf{h}|}{a}\right)^{\nu} K_{\nu}\left(\frac{2\sqrt{\nu}|\mathbf{h}|}{a}\right)\right) & \text{else .} \end{cases} \quad (3)$$

- Comparing the spatial variablity, e.g. the variogram parameter range a and sill b of a sample epoch by varying the number of epochs included in the variogram computation, see Fig. 4(a) and 4(b). Nugget variance c_0 is omitted in this study.
- Evaluating the quality of variogram fitting by computing the root mean squared error (RMSE) and correlation coefficient of the residuals.

Ordinary Kriging Interpolation

- Surface estimation of EZWD by means of Ordinary Kriging, which uses the mathematical function specified with the variogram modell, see Fig. 5
- Evaluating the surface by cross-validation (leave-one-out): remove one GPS data location and predict the associated data using the data at the rest of the locations and compare predicted and measured value by means of RMSE and mean absolute error (MAE)

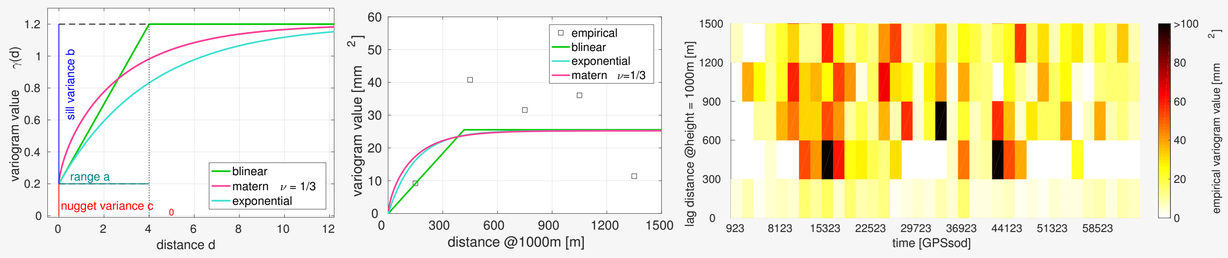

(a) (b) (c)

Fig. 4: General variogram description and three different variogram models used in this study (a), empirical variogram and variogram models fitted to the data of a sample epoch (b) and evolution of empirical variogram over time period of 18h @ 30min.

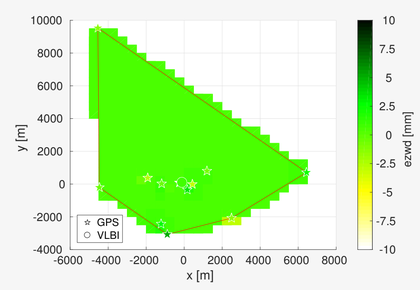

Fig. 5: EZWD surface within convex hull of points from Ordinary Kriging Interpolation with apriori EZWD of GPS and VLBI stations.

Results and Findings

- Number and distribution of EZWDs in a single epoch is not meaningful for fitting a variogram, thus changing the number of epochs included in the variogram for the current epoch: 1s, 5s, 10s, 30s, 1min, 10min, 30min, 1h:

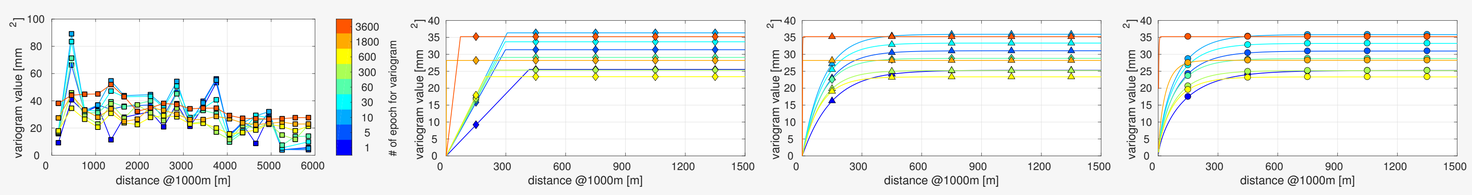

(a) (b) (c) (d)

Fig. 6: Empirical variogram of sample epoch by including different number of observations for the variogram computation of the current epoch (a) and estimated variograms: Linear model (b), Exponential model (c) and Mátern model (d). Note: colorscale is the same for all plots.

- Empirical variogram gets smoother the more epochs are included, but small-scale variations get lost, see Fig. 6
- Three selected variogram models show similar behaviour, no signigicant difference either in the RMSE of the variogram residuals, the correlation coefficient, see Fig. 7 or the estimated variogram parameters, see Fig. 8
- Including more epochs in the variogram computation
  - reduces the RMSE of the variogram residuals and increases the correlation between empirical values and selected model, see Fig. 7
  - decrease the estimated range parameter and increases the estimated sill variance, see Fig. 8

  for the majority of investigated epochs

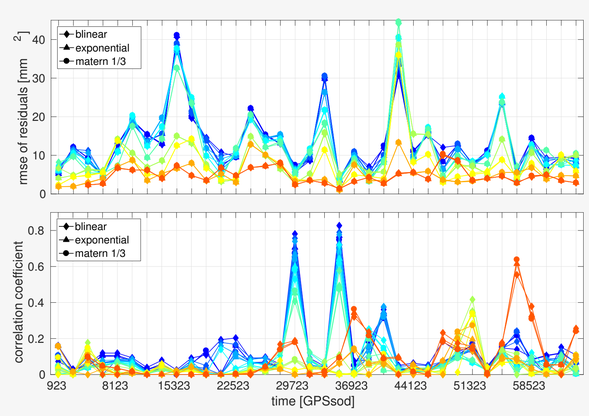

Fig. 7: RMSE of the variogram residuals (top) and correlation coefficient (bottom) between empirical and fitted variogram for three different models. Note: colorscale ist the same as in Fig. 6(a).

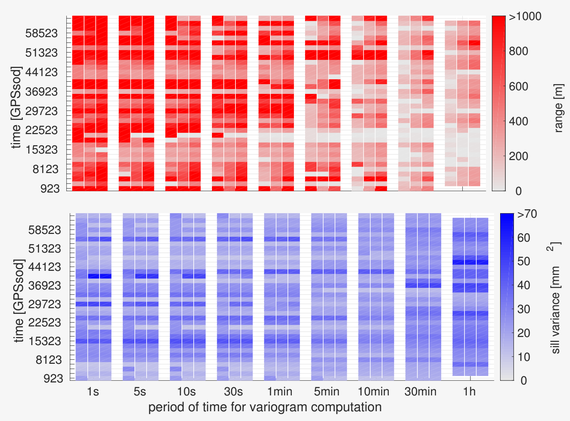

Fig. 8: Estimated variogram parameter range (top) and sill (bottom) for three different models (1st column Linear model, 2nd column Exponential model and 3rd column Mátern model).

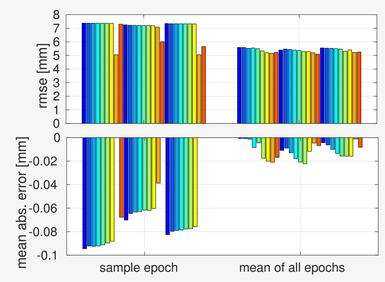

Fig. 9: RMSE (top) and MAE (bottom) for cross-validation (differences EZWD - kriged value) for sample epoch and mean for all epochs (1st column Linear model, 2nd column Exponential model and 3rd column Mátern model). Note: colorscale ist the same as in Fig. 6(a).

- Since variogram fitting shows large residuals, the estimated EZWD surface is to smooth, see Fig. 5.
- Cross-validation: Mean absolute error is negative for all models and epochs in mean, indicating that the kriged EZWDs are a little to big w.r.t. to observed values. The more epochs are included for the variogram estimation, the smaller the rmse of the differences between observed and kriged EZWDs, ses Fig. 9.
- Clustering of points should be considered in future, e.g. by using composed variograms with variable size of lag distances

Acknowledgement

The authors thank the German Research Foundation (DFG) for its financial support (SCHO 1314/3-1), the BKG for the GPS data at Wettzell and Sebastian Halsig from IGG, University of Bonn for VLBI ZWD time series. We further acknowledge the International GNSS Service (IGS) and the Center for Orbit Determination in Europe (CODE) for its products.

Created with LaTeX beamerposter

References

[Fuhrmann et al., 2015] Fuhrmann, T., Luo, X., Knöpfler, A., and Mayer, M. (2015). Generating statistically robust multipath stacking maps using congruent cells. *GPS Solutions*, 19(1):83–92.

[Kube and Schön, 2016] Kube, F. and Schön, S. (2016). PPP Carrier Phase Residual Stacking for Turbulence Investigations, pages 1–7. *Springer Berlin Heidelberg, Berlin, Heidelberg.*

[Stein, 1999] Stein, M. L. (1999). Interpolation of Spatial Data: Some Theory for Kriging. *Springer New York.*

Institut für Erdmessung
Schneiderberg 50
D-30167 Hannover

IGS WORKSHOP 2017 PARIS
PATHWAYS TO IMPROVED PRECISION

IGS Workshop 2017 Paris, France
July 3rd-July 7nd 2017

Franziska Kube
Steffen Schön
www.ife.uni-hannover.de
{kube, schoen}@ife.uni-hannover.de